Continuum Effect in Resonant Excitation Spectra of Weakly-Bound Nuclei

S. J. Dai[a], F. R. Xu[a], J. G. Li[a], B. S. Hu[a] and Z. H. Sun[a,b]

[a] *School of Physics and State Key Laboratory of Nuclear Physics and Technology, Peking University, Beijing 100871, China*

[b] *Physics Division, Oak Ridge National Laboratory, Oak Ridge, Tennessee 37831, USA*

Abstract

Starting from the CD-Bonn potential, we have performed Gamow shell-model calculations for neutron-rich oxygen isotopes, investigating excitation spectra and their resonant properties. The Gamow shell model is based on the Berggren ensemble, which is capable of treating the continuum effect reasonably in weakly-bound or unbound nuclei. To calculate heavier-mass oxygen isotopes, we choose ^{16}O as a frozen core in the Gamow shell-model calculations. The first 2^+ excitation energies of the even-even O isotopes are calculated, and compared with those obtained by the conventional shell model using the empirical USDB interaction. The continuum effect is proved to play an important role in the shell evolution near the drip line. We discuss also the effect of the Berggren contour choice. We improve the approximation in the contour choice to give more precise calculations of resonance widths.

Keywords: *CD-Bonn interaction; Gamow shell model; drip-line nuclei; Berggren ensemble; continuum; resonance*

1 Introduction

Thanks to the radioactive isotope beam technique, the exploration of the neutron drip line is no longer unachievable. A recent experiment performed at RIKEN-RIBF investigated the extremely neutron-rich nucleus ^{26}O by removing a proton from the radioactive secondary beam of ^{27}F [1]. The decay products, ^{24}O and two neutrons, were observed. This experiment confirmed that ^{24}O is the last bound nucleus of neutron-rich oxygen isotopes, and positioned the ground-state resonance of ^{26}O at about 18 keV above threshold. Another excited state in ^{26}O was also observed at 1.28 MeV, which is believed to be the first 2^+ state [1].

As a powerful method for studying atomic nuclei, including in the medium-mass region, the shell model is very commonly used to investigate oxygen isotopes [2–4]. Shell model calculations using the USDB interaction have been successful in reproducing the observables of *sd*-shell nuclei, such as the binding energies, spectra, and transition rates [5–9]. However, the USDB interaction is constructed in the harmonic

Proceedings of the International Conference 'Nuclear Theory in the Supercomputing Era — 2018' (NTSE-2018), Daejeon, South Korea, October 29 – November 2, 2018, eds. A. M. Shirokov and A. I. Mazur. Pacific National University, Khabarovsk, Russia, 2019, p. 183.

http://www.ntse.khb.ru/files/uploads/2018/proceedings/FurongXu.pdf.

oscillator (HO) basis. The HO basis always gives well-localized wave functions of nuclear states. However, these cannot describe the loosely-bound or unbound properties of drip-line nuclei. For the drip-line nucleus ^{26}O, the HO-basis shell-model calculation with the USDB interaction gives a 2^+ excitation energy about 0.8 MeV higher than the experimental data [1]. The three-body model calculations indicate that the two-neutron decay channel may play an important role in the ^{26}O system [10–12].

In the three-body model calculation, the three-body system $^{24}\mathrm{O} + n + n$ is correlated by a density-dependent contact pairing interaction. The two-neutron decay channel is taken into account by evolving the initial state, generated by removing a proton from the calculated ground state of the $^{25}\mathrm{F} + n + n$ system, with the Hamiltonian of the three-body system. The Hamiltonian is based on a one-body Woods–Saxon (WS) potential with a finite depth, and the two-body pairing interaction [10–12]. Using a finite-depth one-body potential is crucial for the model, as it allows the particle emissions.

The three-body model has been successful in reproducing the first 2^+ state energy of ^{26}O, as the decay channel can couple the bound and continuum single particle (s.p.) states [10–12]. For describing the properties of weakly-bound or unbound nuclei near the drip line, the continuum effect has already been proved to be very important [13–19]. In the three-body model, a phenomenological pairing interaction is applied. As was pointed out in Ref. [11], the pairing strength has to be finely tuned to get a precise result. Fitting the pairing strength mixes different effects, like the continuum effect and the three-body force, and the exact contribution from each of them cannot be identified. Another problem is that the three-body model cannot give the decay width directly and the method used to calculate the widths is parameter-dependent [11].

To minimize the obscure mixing effects caused by the fitted interaction, as well as to calculate the decay width self-consistently, we revisit the continuum effect in the oxygen isotopes by the Gamow shell model (GSM) [18, 20, 21] with a realistic nuclear force, the CD-Bonn interaction [22]. The GSM is based on the Berggren ensemble, which is composed of s.p. bound states, resonant states and non-resonant continuums [13, 18, 20, 21]. The continuum states in the Berggren ensemble are analytically extended to the complex plain and discretized along a certain contour. The imaginary parts of the resonant s.p. eigenenergies give the resonance widths of the s.p. states. These s.p. widths integrate to the total widths of the many-body system through the shell model. On the other hand, the CD-Bonn potential describes the nucleon-nucleon interaction with high precision within a very wide range. To accelerate the convergence of many-body calculations, the bare CD-Bonn interaction is renormalized using the $V_{\text{low-}k}$ procedure [23]. For the shell-model calculation with a frozen core, we adopt the Q-box folded-diagram perturbation method [24, 25] to construct a realistic effective model-space Hamiltonian, as done in Ref. [21].

As mentioned above, analytically extending the continuum states to the complex plain is essential in the Berggren ensemble, which includes narrow resonant states, and introduces an additional dimension to describe the resonance width. However, a complex contour requires more discretizing points to reach convergence due to the additional dimension. Since it is believed that the non-resonant continuum mainly couples with bound states through the resonances, and the direct coupling is assumed to be less important, in most models based on the Berggren ensemble, only partial waves that include narrow resonances are extended to the complex plain [18, 20, 21, 26–30].

However the accuracy of this approximation is not yet well tested. In this paper, we will discuss the Berggren contour choice in the oxygen chain by expanding the extended partial waves from $d_{3/2}$ to all *sd* partial waves.

In this paper, we perform a realistic-force GSM calculation for the neutron-rich oxygen isotopes ^{18,20,22,24,25,26}O to study how the continuum effect affects the shell evolution in the drip-line region, as well as to investigate the continuum effect from the non-resonant continuum in partial waves without narrow resonances.

2 Theoretical framework

The Berggren ensemble is a s.p. basis specialized for treating the continuum and resonances. The one-body Schrödinger equation in the complex-k space gives the Berggren states,

$$\frac{d^2u\,(r)}{dr^2} = \left(\frac{l\,(l+1)}{r^2} + \frac{2m}{\hbar^2}V_{WS}(r) - k^2\right)u(r), \tag{1}$$

where V_{WS} is the WS potential with a spin-orbit coupling,

$$V_{WS}(r) = -V_0\,f(r) - 4V_{SO}\frac{1}{r}\frac{df(r)}{dr}\;l\cdot s, \tag{2}$$

where l and s refer to the orbital angular momentum and spin of the particle, respectively, and

$$f(r) = -\frac{1}{1+e^{\frac{r-r_0A^{1/3}}{d}}}. \tag{3}$$

The basis states include bound, resonant and continuum states due to the finite depth of the WS potential. In the present calculations, the parameters of the WS potential are $V_0 = 45.39$ MeV, $r_0 = 1.347$ fm, $d = 0.70$ fm, and $V_{SO} = 18.2$ MeV. The *sd*-shell s.p. energies are -5.31 MeV, -3.22 MeV and $(1.06 - 0.09i)$ MeV for the $0d_{5/2}$, $1s_{1/2}$ bound states and $0d_{3/2}$ resonant orbit, respectively. The values are the same as the universal parameters [31], except that the strength $|V_0|$ is reduced to reproduce the experimental width extracted from ^{17}O [21].

The completeness relation of the Berggren ensemble can be written as

$$\sum_{n\in\{b,d\}} u_n(r,k_n)\,u_n(r',k_n) + \int_{L^+} dk\;v(r,k)\,v(r',k) = \delta(r-r'), \tag{4}$$

where b and d denote the bound states and decaying resonant states respectively, and L^+ denotes the integral contour of the continuum. The contour lies in the complex plain. Only narrow resonances enclosed in the contours are included in the summation of Eq. (4) according to Cauchy's integral theorem. Since the orbital angular momentum in the s.p. Hamiltonian is conserved, the contours of different partial waves may differ. For a partial wave that does not contain narrow resonances, a contour lying on the real-momentum axis is widely used.

The effective interaction in the Berggren ensemble is obtained by performing a Q-box folded-diagram perturbation based on the CD-Bonn interaction. The matrix elements, which are given originally in the HO basis, are projected to the Berggren ensemble by overlapping the Berggren basis wave functions and those of the HO

basis. In the present work, we are using the truncation $N_{\text{shell}} = 22$ for the HO basis. The CD-Bonn interaction is renormalized by the $V_{\text{low-}k}$ procedure before projection to the Berggren ensemble. To minimize the induced three-body force in the $V_{\text{low-}k}$ renormalization, a hard cutoff of $\Lambda = 2.6$ fm^{-1} is chosen. In the Q-box calculation, the starting energy is -6 MeV, which is approximately equal to the average sd-shell s.p. energy of the one-body Woods-Saxon potential.

With the ^{16}O core, the model space of the effective interaction is all sd-shell orbits including bound states $0d_{5/2}$ and $1s_{1/2}$, the narrow resonant state $0d_{3/2}$, and the $d_{3/2}$ non-resonant continuum states on the complex plain. As mentioned above, a real-momentum continuum contour is commonly adopted for partial waves that do not have narrow resonances. Because we are also investigating the continuum effect contributed by partial waves that do not have narrow resonances, the results with different contours in the $s_{1/2}$ and $d_{5/2}$ partial waves are compared. We change these contours from the real-momentum axis to the same as that of the $d_{3/2}$ partial wave. In the calculation, we choose the contour $\{0.0 \to 2.2\}$ (in fm^{-1}) in the real axis and discretize it with 20 discrete points. The complex contour is taken as $\{0.0 \to (0.48 - 0.20i) \to 0.62 \to 2.2\}$ (in fm^{-1}) with 20 discrete points as well.

3 Calculations and discussion

The excitation energy of the first 2^+ excited state is an indicator of the shell gap in the sd shell. In this paper, we calculate the 2_1^+ excitation energies of oxygen isotopes, shown in Fig. 1. We see that both the CD-Bonn GSM and USDB HO-basis SM calculations give good agreement with experimental 2_1^+ excitation energies, especially in the well-bound nuclei ^{18,20,22}O, where both calculations reproduce the data well. This indicates that, although based on a realistic force, the effective interaction in the GSM has the same precision for the well-bound systems as the empirical USDB interaction which fits the data of bound nuclei. However, for the 2_1^+ excitation energy in the unbound ^{26}O, the USDB interaction gives 2.11 MeV which is about 800 keV higher than the experimental data. The CD-Bonn GSM improves the results of calculations significantly (see Fig. 1). Since the effective interaction in GSM is as

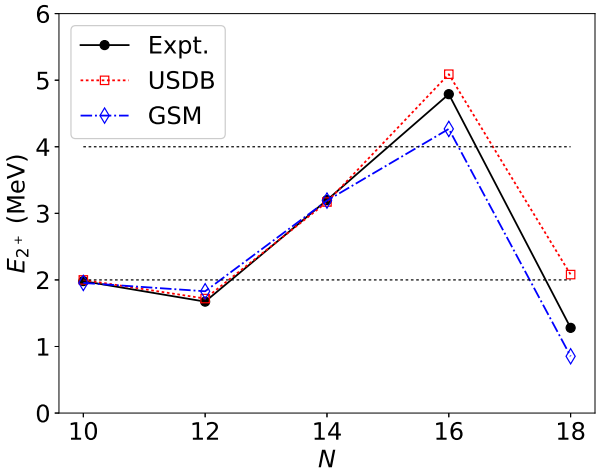

Figure 1: Calculated 2_1^+ excitation energies in ^{18,20,22,24,26}O compared with the experimental data [1, 32] and USDB calculations. The USDB calculation overestimates the 2^+ excitation energy in ^{26}O, while the GSM calculation improves the result by taking the continuum effect into account.

precise as the USDB interaction in the well-bound nuclei, we can thus conclude that the improvement should be mainly due to the inclusion of the continuum.

The calculated 2^+ excitations of ^{24}O and ^{26}O are lower than the experimental data, which may be partially due to the lacking of the three-body force in the GSM calculations. With an increasing number of valence neutrons, the effect of the three-body force becomes significant. In our previous work [21], we proved that the three-body force introduced by the $V_{\text{low-}k}$ process is weak when the hard cutoff of 2.6 fm^{-1} is used. However, the initial three-body force, which is not considered, would have a non-negligible effect for neutron-rich isotopes with a large number of valence neutrons. In the work studying the oxygen chain using the *ab-initio* coupled cluster method [28], with both two-body and three-body interaction derived from the chiral effective field theory [33], the initial three-body force has an effect of increasing the excitation energies of the 2^+ states in the even-even O isotopes. Although the 2^+ state in ^{26}O was not calculated in Ref. [28], the direction of this effect should remain the same. This conclusion supports our result that the 2^+ state is lower in energy than the experimental data if no three-body force is considered.

Another purpose of the present work is to investigate the influence of the contour choice. We use different contours for the *sd* partial waves to calculate all well-bound as well as weakly-bound and unbound nuclei. For convenience, we use the following notations:
i) C_0: the complex contour (i. e., a triangle shape below the real-momentum axis, see Fig. 1 in Ref. [21], our previous paper) with 20 discrete points is employed in the $d_{3/2}$ channel, which contains a narrow resonance, while the real-momentum contours with only 8 discrete points are used in all other channels (including $s_{1/2}$ and $d_{5/2}$ channels), which have no narrow resonances.
ii) C_1: the same as C_0 except that the number of discrete points for $s_{1/2}$ and $d_{5/2}$ partial waves is increased to 20.
iii) C_2: the same as C_1 except that the complex-momentum contour, like that in the $d_{3/2}$ partial wave, is employed in the $s_{1/2}$ channel.
iv) C_3: the same as C_2 except that the same complex-momentum contour employed also in the $d_{5/2}$ channel.

Figure 2 displays the results of calculations of low-lying states in $^{22-26}$O. We see that there is no meaningful changes of the results when the number of discretizing points is increased from 8 to 20, except for the ^{24}O where the energies become slightly lower. An increase in the number of discretizing points leads to a remarkable increase in the model dimension. Therefore, a reasonable but converged number of discretizing points is an issue that one should consider in the GSM calculations. From our calculations for the *sd*-shell nuclei, 8 discretizing points should be reasonable in most cases.

From Fig. 2, we can also analyze the results of calculations with different strategies of the contour choice. Overall, the different strategies in the choices of contours give almost the same results, except that C_3 gives slightly higher energies for the 2^+ and 3^+ states in ^{22}O. This means that for the partial waves with no narrow resonances, real-momentum contours can be chosen without a loss of accuracy of the calculations. A real-momentum contour with reasonable discretizing points can significantly reduce the computational burden. This means that if there are no narrow resonances in the channel, the continuum states on the real-momentum contour are good enough to describe the continuum effect in the real part of the eigenenergies.

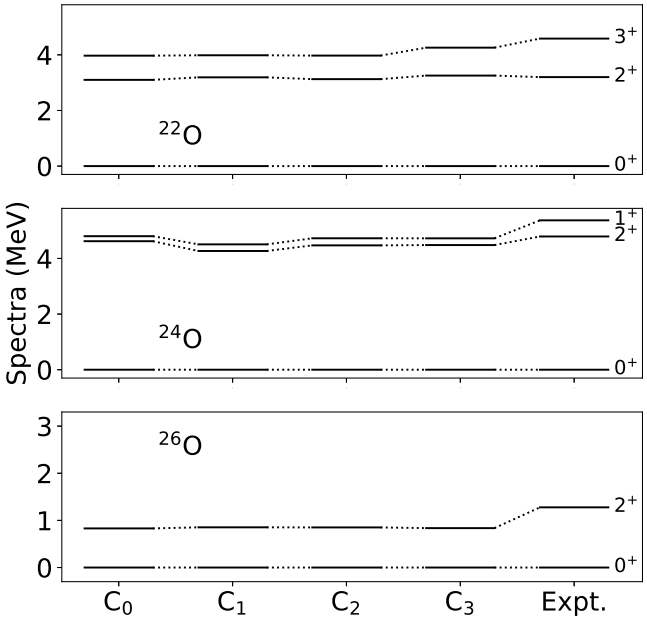

Figure 2: Low-lying states in ^{22,24,26}O. The experimental data are taken from Refs. [1,32]. Different strategies of the contour choosing C_i are defined in the text. The results show that the real parts of the eigenenergies given by GSM do not change meaningfully with the different choices of contours for the channels without narrow resonances.

Figure 3 plots the imaginary parts (i. e., resonance widths) of the obtained eigenenergies of the resonant states in ^{24,25,26}O, compared with the experimental data available currently [1,32]. The calculated resonance widths are gently dependent on the prescriptions of contour choice. The widths tend to be slightly smaller with more partial waves taking complex-momentum contours, and closer to the experimental values. However, the GSM calculation with a complex-momentum contour is much more expensive in computation. The new experiment of ^{26}O [1] mentioned in the

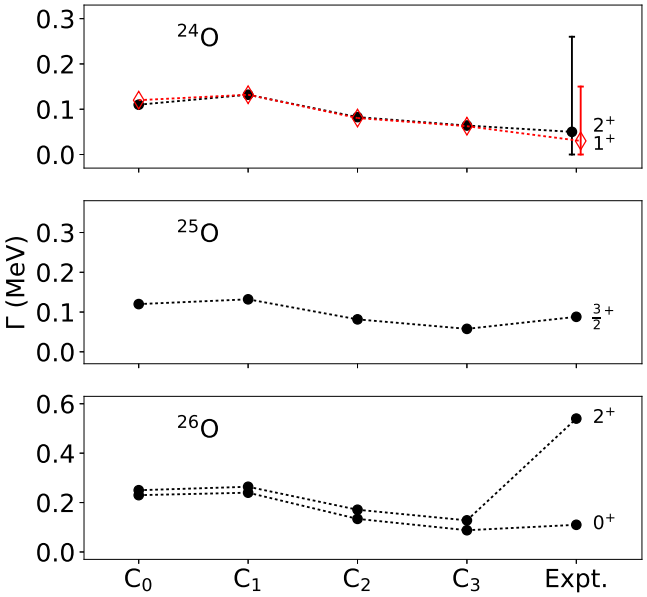

Figure 3: Widths of resonances in ^{24,25,26}O. The experimental data are taken from Refs. [1,32].

introduction has also updated the resonance width of the unbound ^{25}O ground state. The experimental resonance width of the 2^+ state in ^{26}O [1] looks extremely large, much larger than obtained in the GSM calculation. The experimental strength of the 2^+ resonant state is relatively weak, and the FWHM is influenced a lot by continuum states around. The present calculation predicts a much smaller resonance width for this state.

In the present paper, we are investigating how to treat the continuum effect in both energy and width of resonances. For the calculation of resonance energy, choosing a real-momentum contour for a partial wave that has no narrow resonance is good enough to give a convergent result. Taking a complex-momentum contour does not change the result. For the calculation of resonance width, however, choosing complex-momentum contours for all partial waves of the model space seems to be more reasonable, and hence recommended. For partial waves belonging to the excluded space, couplings with valence particles are weak, and hence it should be safe to use real-momentum contours for the respective channels.

4 Conclusion

In conclusion, we have applied the with-core GSM based on the CD-Bonn potential to neutron-rich oxygen isotopes, investigating the continuum effect on both resonance energy and width. These calculations were motivated with the recent experiment on ^{26}O beyond the neutron drip line. The calculated 2^+ excitation energies were compared with shell-model calculations using the empirical USDB interaction, showing a strong continuum effect in the spectra of drip-line nuclei. By choosing the different prescriptions of contours in the Berggren coordinates for the GSM calculation, we have discussed the convergence of the resonance spectrum. It is suggested that all model-space partial waves, regardless of whether there is a narrow resonance, should take the same complex-momentum contour to obtain a convergent resonance width.

5 Acknowledgement

This work has been supported by the National Key R&D Program of China under Grant No. 2018YFA0404401; the National Natural Science Foundation of China under Grants No. 11835001, No. 11575007 and No. 11847203; the China Postdoctoral Science Foundation under Grant No. 2018M630018; and the CUSTIPEN (China-U.S. Theory Institute for Physics with Exotic Nuclei) funded by the U.S. Department of Energy, Office of Science under Grant No. DE-SC0009971.

References

[1] Y. Kondo *et al.*, Phys. Rev. Lett. **116**, 102503 (2016).

[2] E. Caurier, F. Nowacki, A. Poves and J. Retamosa, Phys. Rev. C, **58** 2033 (1998).

[3] C. R. Hoffman *et al.*, Phys. Rev. Lett. **100**, 152502 (2008).

[4] C. Yuan, T. Suzuki, T. Otsuka, F. Xu and N. Tsunoda, Phys. Rev. C **85**, 064324 (2012).

[5] B. A. Brown and W. A. Richter, Phys. Rev. C **74**, 034315 (2006).

[6] M. Kowalska, D. T. Yordanov, K. Blaum, P. Himpe, P. Lievens, S. Mallion, R. Neugart, G. Neyens and N. Vermeulen, Phys. Rev. C **77**, 034307 (2008).

[7] R. Kanungo *et al.*, Phys. Rev. Lett. **102**, 152501 (2009).

[8] K. Tshoo *et al.*, Phys. Rev. Lett. **109**, 022501 (2012).

[9] S. R. Stroberg, H. Hergert, J. D. Holt, S. K. Bogner and A. Schwenk, Phys. Rev. C **93**, 051301(R) (2016).

[10] K. Hagino and H. Sagawa, Phys. Rev. C **90**, 027303 (2014).

[11] K. Hagino and H. Sagawa, Phys. Rev. C **89**, 014331 (2014).

[12] L. V. Grigorenko and M. V. Zhukov, Phys. Rev. C **91**, 064617 (2015).

[13] R. Id Betan, R. J. Liotta, N. Sandulescu and T. Vertse, Phys. Rev. Lett. **89**, 042501 (2002).

[14] K. Bennaceur, J. Dobaczewski and M. Płoszajczak, Phys. Rev. C **60**, 034308 (1999).

[15] N. Michel, W. Nazarewicz and M. Płoszajczak, Phys. Rev. C **82**, 044315 (2010).

[16] I. Rotter, Rep. Prog. Phys. **54**, 635 (1991).

[17] A. Volya and V. Zelevinsky, Phys. Rev. C **74**, 064314 (2006).

[18] N. Michel, W. Nazarewicz, M. Płoszajczak and K. Bennaceur, Phys. Rev. Lett. **89**, 042502 (2002).

[19] W. Fritsch, R. Lipperheide and U. Wille, Nucl. Phys. A **241**, 79 (1975).

[20] N. Michel, W. Nazarewicz, M. Płoszajczak and J. Okołowicz, Phys. Rev. C **67**, 054311 (2003).

[21] Z. H. Sun, Q. Wu, Z. H. Zhao, B. S. Hu, S. J. Dai and F. R. Xu, Phys. Lett. B **769**, 227 (2017).

[22] R. Machleidt, Phys. Rev. C **63**, 024001 (2001).

[23] S. Bogner, T. Kuo and A. Schwenk, Phys. Rep. **386**, 1 (2003).

[24] K. Takayanagi, Nucl. Phys. A **852**, 61 (2011).

[25] N. Tsunoda, K. Takayanagi, M. Hjorth-Jensen and T. Otsuka, Phys. Rev. C **89**, 024313 (2014).

[26] N. Michel, W. Nazarewicz and M. Płoszajczak, Phys. Rev. C **70**, 064313 (2004).

[27] Y. Jaganathen, R. M. I. Betan, N. Michel, W. Nazarewicz and M. Płoszajczak, Phys. Rev. C **96**, 054316 (2017).

[28] G. Hagen, M. Hjorth-Jensen, G. R. Jansen, R. Machleidt and T. Papenbrock, Phys. Rev. Lett. **108**, 242501 (2012).

[29] G. Papadimitriou, J. Rotureau, N. Michel, M. Płoszajczak and B. R. Barrett, Phys. Rev. C **88**, 044318 (2013).

[30] I. J. Shin, Y. Kim, P. Maris, J. P. Vary, C. Forssén, J. Rotureau and N. Michel, J. Phys. G **44**, 075103 (2017).

[31] J. Dudek, Z. Szymański and T. Werner, Phys. Rev. C **23**, 920 (1981).

[32] http://www.nndc.bnl.gov/.

[33] R. Machleidt and D. R. Entem, Phys. Rep. **503**, 1 (2011).